AIMS Mathematics, 9(8): 21860–21889.
DOI: 10.3934/math.20241063
Received: 18 May 2024
Revised: 28 June 2024
Accepted: 03 July 2024
Published: 10 July 2024

http://www.aimspress.com/journal/Math

Research article

A modified Moore-Gibson-Thompson fractional model for mass diffusion and thermal behavior in an infinite elastic medium with a cylindrical cavity

Yazeed Alhassan[1], Mohammed Alsubhi[2] and Ahmed E. Abouelregal[1,3,*]

[1] Department of Mathematics, College of Science, Jouf University, Sakaka 2014, Saudi Arabia
[2] Department of Mathematics, College of Science, Taibah University, Al-Madinah Al-Munawarah, Saudi Arabia
[3] Department of Mathematics, Faculty of Science, Mansoura University, Mansoura 35516, Egypt

* **Correspondence:** Email: ahabogal@ju.edu.sa.

Abstract: This article discussed a new fractional model that included governing equations describing mass and thermal diffusion in elastic materials. We formulated the thermal and mass diffusion equations using the Atangana-Baleanu-Caputo (ABC) fractional derivative and the Moore-Gibson-Thomson (MGT) equation. In addition to the fractional operators, this improvement included incorporating temperature and diffusion relaxation periods into the Green and Naghdi model (GN-III). To verify the proposed model and analyze the effects of the interaction between temperature and mass diffusion, an infinite thermoelastic medium with a cylindrical hole was considered. We analyzed the problem under boundary conditions where the concentration remained constant, the temperature fluctuated and decreased, and the surrounding cavity was free from any external forces. We applied Laplace transform techniques and Mathematica software to generate calculations and numerical results for various field variables. We then compared the obtained results with those from previous relevant models. We have graphically depicted the results and extensively examined and evaluated them to understand the effects of the relationship between temperature and mass diffusion in the system.

Keywords: fractional derivative; thermoelastic; diffusion; MGT equation; infinite medium
Mathematics Subject Classification: 74F05, 74F10, 74F15

1. Introduction

Thermoelasticity theory, a prominent field in solid mechanics, investigates the interaction between thermal and mechanical phenomena in materials. The theory acknowledges that temperature fluctuations can lead to changes in shape and internal forces in a material, and vice versa, applying mechanical forces can result in temperature alterations [1]. Thermoelasticity theory is based on the idea that temperature fluctuations cause changes in a material's internal structure and properties, resulting in thermal strains and stresses. Thermoelasticity theory has a variety of applications in engineering. The design of structures and components that experience temperature fluctuations is an essential consideration. Engineers can improve the performance of their designs by understanding how materials react to thermal and mechanical loads, which allows them to predict and prevent possible problems [2]. The aerospace industry uses thermoelasticity theory to design aircraft components that can withstand the significant temperature variations encountered during flight [3]. Civil engineers also use thermoelasticity theory to design structures such as bridges and pipelines that are subject to temperature fluctuations. Moreover, it holds significance in the examination of thermal strains in electronic devices and microelectromechanical systems (MEMS). These fields benefit from understanding the impact of temperature fluctuations on the mechanical properties and dependability of the materials and components in question [4].

The conventional coupled thermoelasticity (CTE) theory, as proposed by Biot [5], is subject to certain unrealistic constraints because it assumes that heat can propagate at an infinite velocity. Several alternative thermoelasticity models, known as generalized thermoelasticity, have emerged to resolve this issue. These models have garnered substantial scientific attention in recent years. Lord and Shulman [6] developed a theory by altering the heat conduction equation to include the heat flow rate. They developed an expanded thermoelasticity theory integrating a thermal flux rate alongside the conventional Fourier heat conduction law. Furthermore, Green and Lindsay [7] developed a theory incorporating the temperature rate as a fundamental component. In their hypothesis, they introduced two relaxation periods, which modified the energy equation and established the relationship between Duhamel and Neumann. Following this, the work of Green and Naghdi [8–10] garnered significant interest as they formulated three distinct forms of generalized (GN) thermoelasticity theory, stimulating further research in this field. The initial theory is referred to as GN-I, the subsequent theory as GN-II, and the final theory as GN-III. In its linearized form, the GN-I theory aligns with the traditional heat conduction equation. The GN-II model does not involve any loss of thermal energy. Instead, it introduces an alternative equation for heat conduction that addresses the issue of infinite propagation of heat waves in thermoelasticity.

The field of acoustics and wave propagation frequently uses the Moore-Gibson-Thompson (MGT) equation, a third-order differential equation. It is notably used to model situations where dissipation and dispersion play important roles. Its higher-order nature allows it to represent more complex dynamic behaviors than classic second-order wave equations, such as those found in standard thermoelasticity and acoustics [11]. Quintanilla [12,13] introduced a unique thermoelastic model featuring two temperatures, incorporating the MGT version for heat conduction. This model was developed from the GN-III theory, with the addition of a relaxation component. Quintanilla's model includes a relaxation factor [14]. This new model exhibits additional dynamics and properties that go beyond those seen in standard thermoelasticity models. The introduction of the MGT has had a substantial impact on the field of thermoelasticity. This model has attracted a wider variety of

researchers and has stimulated further inquiries into the theory and its applications [15–18]. Ahmed et al. [19] developed a singular boundary approach, often referred to as SBM, to solve transient, dynamically coupled thermoelastic issues. The Helmholtz decomposition and eigenvalue analysis in the frequency domain (Fourier space) are used to obtain novel fundamental solutions to dynamically coupled thermoelastic issues.

Mass diffusion refers to the movement of atoms, molecules, or other species within a porous material due to concentration differences. It involves transferring mass from areas of higher concentration to areas of lower concentration. The random movement and collisions of particles within a medium cause mass diffusion [20]. The concentration gradient, species diffusivity, and environmental conditions are some of the factors that affect the rate of mass diffusion. Elastic materials link the processes of heat diffusion and mass diffusion. Sometimes, temperature differences can cause concentration differences, a phenomenon known as thermodiffusion, or the Soret effect. Under the influence of a temperature gradient, this effect causes different species to move through the material more rapidly [21]. Understanding how heat and mass move through elastic materials is important in many fields, such as physics, materials science, and engineering. It is a key component of many processes, including heat transfer, mass transport, phase changes, and diffusion-based methods for characterizing materials [22].

In semiconductor production, thermal diffusion is used to establish precise doping profiles in semiconductor materials. Dopant atoms must be carefully diffused into silicon or other semiconductor substrates to alter the electrical properties of transistors, diodes, and other electronic devices [23]. Thermal and mass diffusion play crucial roles in processes such as diffusion coating and surface modification. These processes enhance the characteristics of a substrate material by diffusing a thin layer of another material onto its surface. Diffusion occurs when carbon penetrates the outer layer of steel, forming a tough, carbon-rich layer known as the carburized layer. This process enhances the steel's resistance to wear and tear. Thermal diffusion is widely employed in heat treatment processes, including annealing, tempering, and quenching [24]. These processes involve the deliberate application of heat and cold to manipulate the internal structure and characteristics of materials. Thermal diffusion is essential for establishing the required temperature profiles and managing phase transitions within the material.

Nowacki introduced the concept of thermoelastic diffusion [25]. This concept introduces a novel thermoelastic model that necessitates the transmission of thermoelastic waves at infinite speeds. Sherief et al. [26] proposed a generalized thermoelastic model indicating restricted velocities for the propagation of thermoelastic and thermal waves.

This article describes a new model for mass and thermal diffusion based on the MGT fractional thermodiffusion theory. It demonstrates how thermoelasticity and mass diffusion interact. The purpose of this model is to rectify the shortcomings of prior models and enhance our understanding of thermodiffusion. This new model includes the fractional MGT equation, which provides an accurate description of heat conduction and diffusion in elastic materials. The equation is derived using the fractional Atangana-Baleanu-Caputo (ABC) derivative, which incorporates a nonlocal and non-anomalous kernel. Using fractional derivatives allows the inclusion of memory effects, which effectively explain why thermal and mass waves propagate at finite speeds. Additionally, this proposed model accounts for the restricted speeds at which thermal and mass waves can propagate. This differs from the assumptions made in conventional Fourier models and the third form of GN theory. The goal of this new model is to address the limitations of previous theories by incorporating fractional

derivatives. This approach will result in a more precise and comprehensive depiction of thermodiffusion in elastic materials.

To examine the proposed model, the study focused on investigating thermal diffusion interactions in an infinitely large isotropic material with a cylindrical hole. This problem assumes that both time-dependent heat transfer and chemical convection affect the surface of the cylindrical hollow, which offers no resistance to movement. The problem was analyzed using the Laplace transform approach. The Laplace transform was used to derive analytical expressions for the system's physical fields, such as temperature and concentration. After obtaining the solutions in the Laplace domain, an appropriate numerical inversion procedure was used to transform the solutions back to the space-time domain. To verify the accuracy of the model and compare it with other established models, we computed the numerical values of the physical fields and displayed them in figures and tables. We verified the efficacy and distinctiveness of the proposed model in describing thermal diffusion interactions in the analyzed system by computing numerical values for the physical fields depicted in figures. This comparison also facilitated the assessment of the efficacy of the proposed model, as well as its congruence with preceding theories and empirical evidence.

Nomenclature:

λ, μ	Lamé′s constants	K	Thermal conductivity
α_t	thermal expansion coefficient	ρ	Density of material
α_c	coefficient of linear diffusion	Q	Heat source
$\beta_1 = (3\lambda + 2\mu)\alpha_t$	thermal coupling	$\beta_2 = (3\lambda + 2\mu)\alpha_c$	Diffusion coupling
T_0	environmental temperature	δ_{ij}	Kronecker′s delta function
$\theta = T - T_0$	temperature increment	∇^2	Laplacian operator
T	absolute temperature	τ_0	Phase lag of heat flux
C_E	Specific heat	$\vec{\mathcal{P}}$	Position vector
$e = \varepsilon_{kk} = \nabla \cdot \vec{\mathrm{u}}$	cubical dilatation	τ_η	Phase lag of diffusing mass
σ_{ij}	Stress tensor	a	measure of thermoelastic diffusion effect
ε_{ij}	Strain tensor	α	Fractional order
$\vec{\mathrm{u}}$	Displacement vector	D	Thermodiffusion coefficient
$\vec{\mathrm{H}}$	Heat flux vector	P	Chemical potential
$\vec{\eta}$	Diffusing mass vector	C	Concentration of diffusion material

2. Fractional MGT thermodiffusion model

Mathematics, physics, and engineering frequently employ Fourier and Fick's formulas to explain the processes of thermal conduction and mass diffusion in elastic materials. Nevertheless, these models may exhibit deficiencies or imperfections that do not consistently align with experimental observations. In this section, we will develop a novel model that overcomes the restrictions and offers a more comprehensive understanding of heat transfer and diffusion phenomena. The model incorporates the MGT equation and utilizes fractional-order differential operators.

The equations and relationships that describe how generalized thermodiffusion works in uniform, isotropic, elastic solids are based on the laws of conservation of energy, momentum, and mass. They also look at the relationships between stress, strain, heat flux, and mass flux. The principles of thermodynamics and continuum mechanics commonly represent these equations as partial differential equations. The following equations regulate the thermodiffusion behavior of elastic solids [23–26]:

$$\vec{H}(\vec{\mathcal{P}},t) = -K\nabla\theta(\vec{\mathcal{P}},t), \tag{1}$$

$$\vec{\eta}(\vec{\mathcal{P}},t) = -D\nabla P(\vec{\mathcal{P}},t), \tag{2}$$

$$\varepsilon_{ij} = \frac{(u_{j,i}+u_{i,j})}{2}, \tag{3}$$

$$\rho C_e \frac{\partial\theta}{\partial t} + \beta_1 T_0 \frac{\partial}{\partial t}(\nabla\cdot\vec{\mathrm{u}}) + aT_0\frac{\partial C}{\partial t} = -\nabla\cdot\vec{\mathrm{H}} + Q, \tag{4}$$

$$-\nabla\cdot\vec{\eta} = \dot{C}, \tag{5}$$

$$P = -\beta_2\varepsilon_{kk} + bC - a\theta. \tag{6}$$

Equations (1)–(6) allow prediction of the behavior of the material under different loading and temperature conditions. In addition, they allow for the analysis of the effect of thermodiffusion on the solid's mechanical response.

The conventional laws of Fourier and Fick, which govern heat transfer and diffusion, have been extensively employed and validated for several practical applications. Nevertheless, these principles fail to precisely represent the patterns of temperature fluctuations in the short-term period, especially at higher frequencies and smaller wavelengths. In order to overcome this constraint and rectify the incongruity with physical events, generalized equations have been formulated. Over the last thirty years, nonclassical diffusion and thermal elasticity models have been superseded by more comprehensive equations designed to address this discrepancy. A specific model that incorporates thermodiffusion with a relaxation time is the generalized model established by Sherief et al. [26]. This model incorporates a relaxation time parameter to facilitate the attenuation of thermal wave propagation.

Notably, the Cattaneo equation, a modified version of the heat equation, frequently replaces the conventional Fourier's law of heat conduction [27]. It provides a more complete picture of heat transport by considering the finite speed of thermal waves and capturing events that the standard Fourier equation does not adequately explain. The modified Cattaneo equation can be written as follows [27,28]:

$$\left(1+\tau_0\frac{\partial}{\partial t}\right)\vec{H}(\vec{\mathcal{P}},t) = -K\nabla\theta(\vec{\mathcal{P}},t), \tag{7}$$

where τ_0 denotes the characteristic relaxation time constant.

An expression resembling the Cattaneo equation is provided, but it is applicable to diffusive mass or mass flow as opposed to heat transfer. The formulation is as follows [26]:

$$\left(1+\tau_1\frac{\partial}{\partial t}\right)\vec{\eta}(\vec{\mathcal{P}},t) = -D\nabla P(\vec{\mathcal{P}},t), \tag{8}$$

where τ_1 represents the relaxation parameter for diffusion time. The relaxation times (τ_0 and τ_1) in thermodiffusion models show how long it takes for a material to reach a new state of equilibrium after changes in temperature or other thermodynamic variables. These relaxation periods are frequently

included in the governing equations of the models to accurately represent the time-dependent behavior of the systems.

Green and Naghdi [16,17] introduced a novel thermoelastic theory that incorporates a constituent function ψ. This function represents the gradient of thermal displacement and is considered the mechanical displacement counterpart in thermal fields. In the GN-III model, the equation that describes the law of enhanced heat transfer is as follows [16]:

$$\vec{H}(\vec{\mathcal{P}},t) = -K\nabla\theta(\vec{\mathcal{P}},t) - K^*\nabla\psi(\vec{\mathcal{P}},t), \tag{9}$$

where the function ψ is taken to satisfy the equation $\theta = \partial\psi/\partial t$ and K^* represents a positive constant feature of the material that is known as the heat conductivity rate.

Abouelregal [29–31] proposed a relation that is analogous to this one for the diffusion mass vector, which may be expressed as follows:

$$\vec{\eta}(\vec{\mathcal{P}},t) = -D\nabla P(\vec{\mathcal{P}},t) - D^*\nabla\phi(\vec{\mathcal{P}},t), \tag{10}$$

where the function ϕ is the chemical displacement gradient to satisfying the relation $P = \partial\phi/\partial t$ and the parameter D^* represents the diffusion rate factor.

It was discovered that the same defect in the traditional Fourier hypothesis, which states that thermal conduction waves propagate instantaneously, also occurs when the modified Fourier law (9) is combined with the energy equation (4). To address this problem using the MGT equation, Quintanilla [12] updated this suggestion in a general sense and integrated a relaxation time into the Green-Lunge model of the third form. Quintanilla incorporated the following modification [12]:

$$\left(1 + \tau_0 \frac{\partial}{\partial t}\right)\vec{H}(\vec{\mathcal{P}},t) = -K\nabla\theta(\vec{\mathcal{P}},t) - K^*\nabla\psi(\vec{\mathcal{P}},t). \tag{11}$$

A differentiation of Eq (11) yields the following:

$$\left(1 + \tau_0 \frac{\partial}{\partial t}\right)\frac{\partial\vec{H}(\vec{\mathcal{P}},t)}{\partial t} = -K\frac{\partial}{\partial t}\nabla\theta(\vec{\mathcal{P}},t) - K^*\nabla\psi(\vec{\mathcal{P}},t). \tag{12}$$

By applying symmetry, the mass flow equation (10) can be refined to have the following structure, similar to how Eq (11) was derived.

$$\left(1 + \tau_1 \frac{\partial}{\partial t}\right)\vec{\eta}(\vec{\mathcal{P}},t) = -D\nabla P(\vec{\mathcal{P}},t) - D^*\nabla\phi(\vec{\mathcal{P}},t). \tag{13}$$

When we differentiate the previous relationship, we arrive to the following:

$$\left(1 + \tau_1 \frac{\partial}{\partial t}\right)\frac{\partial\vec{\eta}(\vec{\mathcal{P}},t)}{\partial t} = -D\frac{\partial}{\partial t}\nabla P(\vec{\mathcal{P}},t) - D^*\nabla\phi(\vec{\mathcal{P}},t). \tag{14}$$

The applications of fractional order derivatives in diffusion equations have increased significantly in recent years. Fractional diffusion equations now come in a wide variety of forms, including the fractional diffusion-reaction equation [32], the fractional sub-diffusion equation [33], and the fractional dispersion equation [34]. Although the Caputo fractional derivative [35] has been widely applied in various fields, its singular kernel is a significant drawback. Atangana and Baleanu [36,37] modified the kernel to address this issue. The new definition proposed by Atangana

and Baleanu, with its non-singular and nonlocal kernel, has advantages over Caputo's definition, especially in physics problems involving initial values. Following this revised definition, significant work has been carried out, including contributions by Atangana and Koca [38] on the existence and uniqueness of solutions to fractional systems. Numerous researchers have demonstrated the practicality of using the Atangana-Baleanu-Caputo (ABC) derivative in real-world applications. The Caputo fractional derivative of a function $\hbar(t)$ with order α, represented as $D_t^{(\alpha)}$, is defined in the following manner:

$$ {}_0^C D_t^{(\alpha)} \hbar(t) = \frac{1}{\Gamma(1-\alpha)} \int_0^t \dot{\hbar}(\tau)(t-\tau)^{-\alpha}\, d\tau, \quad 0 < \alpha < 1. \tag{15} $$

The ABC derivative for a function $\hbar(t)$, of order $\alpha \in (0,1]$ is defined as the following form

$$ {}^{ABC}_0 D_t^{(\alpha)} \hbar(t) = \frac{M(\alpha)}{1-\alpha} \int_0^t \dot{\hbar}(\tau) E_\alpha \left(-\frac{\hat{\alpha}}{1-\alpha}(t-\tau)^\alpha \right) d\tau, \tag{16} $$

where $M(\alpha)$ is a normalization function such that $M(1) = M(0) = 1$ and $E_\alpha(\cdot)$ denotes the Mittag-Leffler function with one parameter. Also, the value of $\hat{\alpha}$ is determined by α/t_0, while t_0 represents the standard unit of time [39,40]. However, they ultimately determined that $\hat{\alpha} = \alpha$.

The current work presents an extension of the MGT model by incorporating the fractional derivative into Eqs (13) and (14). This generalization allows for the description of the nonlocal effects and memory effects of thermal conduction phenomena. By choosing the correct fractional derivative factor and the value of the fractional order parameter α, it is possible to capture different types of temporal behavior, such as sub-diffusion and super-diffusivity. Thus, this makes it possible to obtain a more accurate description of heat conduction processes in complex materials and applications. Within the framework of this proposal, the standard integer-order time derivative $\partial/\partial t$ is substituted by the fractional ABC derivative operator $D_t^{(\alpha)}$, where $0 < \alpha < 1$. Therefore, the following modifications can be made to Eqs (12) and (14):

$$ \left(1 + \tau_0^\alpha\, D_t^{(\alpha)}\right) \frac{\partial \vec{H}(\vec{\mathcal{P}},t)}{\partial t} = -K \frac{\partial}{\partial t} \nabla\theta\left(\vec{\mathcal{P}},t\right) - K^* \nabla\psi\left(\vec{\mathcal{P}},t\right), \tag{17} $$

$$ \left(1 + \tau_1^\alpha\, D_t^{(\alpha)}\right) \frac{\partial \vec{\eta}(\vec{\mathcal{P}},t)}{\partial t} = -D \frac{\partial}{\partial t} \nabla P\left(\vec{\mathcal{P}},t\right) - D^* \nabla\phi\left(\vec{\mathcal{P}},t\right). \tag{18} $$

One may get a modified fractional heat conduction equation by combining the energy equation (4) with the MGT heat equation (17):

$$ \frac{\partial}{\partial t}\left(1 + \tau_0^\alpha\, D_t^{(\alpha)}\right)\left(\frac{\partial}{\partial t}(\rho C_e \theta + \beta_1 T_0 e + a T_0 C) - Q\right) = \left(K \frac{\partial}{\partial t} + K^*\right) \nabla^2 \theta. \tag{19} $$

The modified fractional MGT equation of mass diffusion can be obtained by applying the divergence operator to Eq (18) and utilizing Eqs (5) and (6):

$$ \left(1 + \tau_1^\alpha\, D_t^{(\alpha)}\right) \frac{\partial^2 C}{\partial t^2} = \left(D \frac{\partial}{\partial t} + D^*\right) \nabla^2 (b\, C - a\, \theta - \beta_2\, \varepsilon_{kk}\,). \tag{20} $$

In order to finalize the system of equations that regulate thermal transfer and diffusion in homogeneous bodies with isotropic properties, the constitutive and equation of motion equations, respectively, will be presented:

$$ \mu u_{i,jj} + (\lambda + \mu) u_{j,ij} + F_i = \rho \ddot{u}_i + \beta_1 \theta_{,i} + \beta_2 C_{,i}, \tag{21} $$

$$\sigma_{ij} = 2\mu\varepsilon_{ij} + \delta_{ij}\lambda\varepsilon_{kk} - \delta_{ij}(\beta_1\theta + \beta_2 C). \quad (22)$$

The equations presented in this part establish a structure for studying the interconnected relationship between mechanical deformation, heat transfer, and diffusion in materials. In diverse engineering and scientific contexts, such as examining the behavior of materials under thermal and mechanical stress, investigating diffusion processes, and designing structures with specific thermal and diffusion characteristics, this system of equations facilitates a thorough comprehension of the material's reaction.

3. Special cases

When the generalized fractional equations for thermal conduction (19) and mass diffusion (20) are considered, general models of thermoelasticity with and without diffusion and fractional derivative operators can be obtained. Some special cases can be summarized as follows:

3.1. In the absence of the diffusion influence and fractional derivatives

Without considering the effects of diffusion influence and fractional derivatives ($C, P = 0$ and $\alpha = 1$), the following models can be derived:

- Biot's thermoelastic theory (CTE) [5] at $K^* = 0$ and $\tau_0 = 0$.
- Lord-Shulman theory with a thermal relaxation time (LS) discussed in [6] at $K^* = 0$.
- Thermoelasticity without energy dissipation (GN-III) [10] at $\tau_0 = 0$.
- Thermoelasticity with energy dissipation (GN-II) [9] when $\tau_0 = 0$ and the term $K\frac{\partial}{\partial t}$ is absent.
- Moore-Gibson-Thompson thermoelastic model (MGT-TE) [15,17] when $K^*, \tau_0 > 0$.

3.2. Without fractional derivatives and considering the diffusion effect

When heat transfer and mass diffusion are considered, the generalized model proposed in this case allows the study of coupled phenomena involving both thermal and concentration fields. This is applicable in cases where there is simultaneous transfer of heat and mass diffusion, such as in chemically reactive systems or multiphase materials. By accounting for diffusion and excluding fractional derivatives ($\alpha = 1$), it is possible to construct five thermodiffusion models that are like the previous ones. These models are represented as CTE-D, LS-D, GN-II-D, GN-III-D, and MGT-TE-D.

3.3. When diffusion influences and fractional derivatives are present

By considering the diffusion effect and fractional differential derivatives, we can create five other thermoelastic models like the ones above designated as CTE-FD, LS-FD, GN-II-FD, GN-III-FD, and MGT-TE-FD.

4. Application to the proposed model

We studied a thermo-diffusive material with an unbounded dimension and a cylinder-shaped hole (see Figure 1). A cylindrical coordinate system (r, Θ, z) with the z-axis aligned with the cylinder axis

will be considered for the study's purposes. The regularity condition will be considered to ensure that the values of all the variables that make up the physical field, such as temperature, concentration, and displacement, disappear as r approaches infinity. At time $t = 0$, the elastic medium will be at rest, with an initial concentration of C_0 and a temperature of T_0. It was assumed that there were no external forces or sources affecting the elastic material.

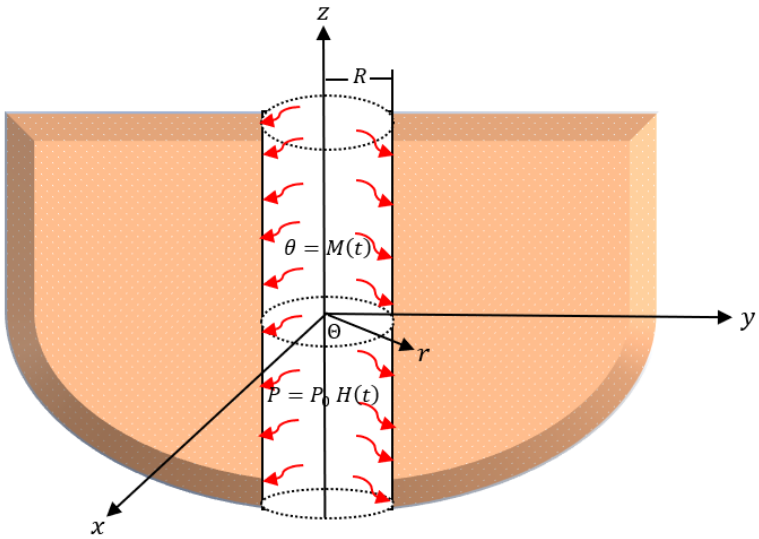

Figure 1. Schematic diagram of an infinite thermally diffusive medium with a cylinder-shaped gap.

Based on the problem assumptions, the components of the displacement and strain tensor can be determined as follows:

$$u_r = u(r,t), \;\; u_\Theta = 0 = u_\varphi, \tag{23}$$

$$\varepsilon_{rr} = \frac{\partial u}{\partial r}, \quad \varepsilon_{\Theta\Theta} = \frac{u}{r}, \;\; \varepsilon_{zz} = \varepsilon_{rz} = \varepsilon_{r\Theta} = \varepsilon_{\Theta z} = 0. \tag{24}$$

From Eq (21), we can get the cubical expansion as:

$$e = \varepsilon_{rr} + \varepsilon_{\varphi\varphi} + \varepsilon_{\Theta\Theta} = \frac{\partial u}{\partial r} + \frac{u}{r}. \tag{25}$$

With the help of Eqs (22) and (6), the radial and hoop stresses, as well as the chemical potentials, can be written by the following relations:

$$\sigma_{rr} = 2\mu\frac{\partial u}{\partial r} + \lambda\left(\frac{\partial u}{\partial r} + \frac{u}{r}\right) - \beta_1\theta - \beta_2 C, \tag{26}$$

$$\sigma_{\Theta\Theta} = \lambda\left(\frac{\partial u}{\partial r} + \frac{u}{r}\right) + 2\mu\frac{u}{r} - \beta_1\theta - \beta_2 C, \tag{27}$$

$$P = bC - a\theta - \beta_2 e. \tag{28}$$

The modified MGT fractional heat transfer equation (19) and the modified MGT fractional diffusion of mass equation (20) can be described by the following equations:

$$\frac{\partial}{\partial t}\left(1+\tau_0^{\alpha}\, D_t^{(\alpha)}\right)\left(\frac{\partial}{\partial t}(\rho C_e\theta+\beta_1 T_0 e+aT_0 C)-Q\right)=\left(K\frac{\partial}{\partial t}+K^*\right)\nabla^2\theta, \tag{29}$$

$$\left(1+\tau_1^{\alpha}\, D_t^{(\alpha)}\right)\frac{\partial^2 C}{\partial t^2}=\left(D\frac{\partial}{\partial t}+D^*\right)\nabla^2(b\,C-a\,\theta-\beta_2\,\varepsilon_{kk}). \tag{30}$$

In the context of cylindrical coordinates and radial symmetry, the Laplacian operator ∇^2 can be represented as follows:

$$\nabla^2=\frac{\partial^2}{\partial r^2}+\frac{1}{r}\frac{\partial}{\partial r}. \tag{31}$$

The motion equation (21) can be written as follows when considering cylindrical coordinates:

$$\sigma_{rr,r}+\frac{1}{r}(\sigma_{rr}-\sigma_{\Theta\Theta})=\rho\frac{\partial^2 u}{\partial t^2}. \tag{32}$$

When we substitute Eqs (26) and (27) into Eq (32), we get the following differential equation:

$$\left[\frac{\partial^2}{\partial r^2}+\frac{1}{r}\frac{\partial}{\partial r}-\frac{1}{r^2}-\frac{1}{c_1^2}\frac{\partial^2}{\partial t^2}\right]u=\frac{\rho\beta_1}{c_1^2}\frac{\partial\theta}{\partial r}+\frac{\rho\beta_2}{c_1^2}\frac{\partial C}{\partial r},\ c_1^2=\frac{\lambda+2\mu}{\rho}. \tag{33}$$

The result obtained by applying the cylindrical divergence operator $(\nabla\cdot)$ to both sides of Eq (33) is as follows:

$$\left[\nabla^2-\frac{1}{c_1^2}\frac{\partial^2}{\partial t^2}\right]e=\frac{\rho\beta_1}{c_1^2}\nabla^2\theta+\frac{\rho\beta_2}{c_1^2}\nabla^2 C. \tag{34}$$

For the purpose of simplifying the governing equations in a form that is more convenient, the dimensionless variables that are listed below can be utilized:

$$\begin{gathered}(r',u')=c_1\eta(r,u),\ (\ t',\tau_0',\tau_1')=c_1^2\eta(\ t',\tau_0,\tau_1),\eta=\frac{\rho C_E}{K},\\ \sigma_{ij}'=\frac{\rho}{c_1^2}\sigma_{ij},\theta'=\frac{\rho\beta_1}{c_1^2}\theta,\ \ P'=\frac{1}{\beta_2}P,\quad C'=\frac{\rho\beta_2}{c_1^2}C.\end{gathered} \tag{35}$$

By introducing these dimensionless quantities, the basic equations can be written as follows:

$$\left(\nabla^2-\frac{\partial^2}{\partial t^2}\right)e=\nabla^2(\theta+C), \tag{36}$$

$$\frac{\partial^2}{\partial t^2}\left(1+\tau_0^{\alpha}\, D_t^{(\alpha)}\right)[\theta+\varepsilon e+\eta_1 C]=\left(\frac{\partial}{\partial t}+\gamma_1\right)\nabla^2\theta, \tag{37}$$

$$\left(\frac{\partial}{\partial t}+\gamma_2\right)\nabla^2(\eta_3\,C-\ e-\eta_4\theta\ )=\eta_2\left(1+\tau_1^{\alpha}\, D_t^{(\alpha)}\right)\frac{\partial^2 C}{\partial t^2}, \tag{38}$$

$$\sigma_{rr}=\xi_1 e+\xi_2\frac{\partial u}{\partial r}-(\theta+C), \tag{39}$$

$$\sigma_{\Theta\Theta}=\xi_1 e+\xi_2\frac{u}{r}\ -(\theta+C), \tag{40}$$

$$P = \eta_3 C - e - \eta_4 \theta, \tag{41}$$

where

$$\begin{gathered}\eta_1 = \frac{a\beta_1 T_0}{\eta K \beta_2}, \eta_4 = \frac{a\rho c_1^2}{\beta_1 \beta_2} \quad \eta_2 = \frac{\rho c_1^2}{\beta_2^2 \eta D}, \eta_3 = \frac{b\rho c_1^2}{\beta_2^2}, \varepsilon = \frac{\beta_1^2 T_0}{\rho^2 c_E c_1^2}, \\ \gamma_1 = \frac{K^*}{\rho C_E K}, \gamma_2 = \frac{D^*}{\beta_2 D}, \xi_1 = \frac{\lambda}{\lambda+2\mu}, \xi_2 = \frac{2\mu}{\lambda+2\mu}.\end{gathered} \tag{42}$$

For the sake of simplicity, we have decreased the primes in Eqs (36) through (41).

5. Initial and boundary conditions

To find a solution to this problem, we will take into account the initial conditions. This is the initial state of the system when $t = 0$. It is initially assumed that the displacement, temperature, and concentration variables are all equal to zero, and that their time derivatives are also equal to zero. Then, the initial conditions can be written as:

$$u = 0 = \frac{\partial u}{\partial t}, \quad \theta = 0 = \frac{\partial \theta}{\partial t}, \quad C = 0 = \frac{\partial C}{\partial t}, \; t = 0. \tag{43}$$

The traction-free limits and varying temperature of the decomposing surface of the inner cylinder bore will be taken into account. In addition, we assumed a possible chemical shock and a sudden change in the chemical potential on the cavity surface. As a result, the boundary condition on the inner surface of the cavity ($r = R$) can be expressed as follows:

$$\sigma_{rr} = 0 \qquad \text{at} \quad r = R, \tag{44}$$

$$\theta = M(t) = \theta_0 t \cos(t)\, e^{-\delta t/2} \qquad \text{at} \quad r = R, \tag{45}$$

$$P = P_0\, H(t) \qquad \text{at} \quad r = R, \tag{46}$$

where θ_0 and P_0 are assumed to be constants, δ is the decay rate constant, and $H(t)$ is the Heaviside unit step function.

6. Solution in the Laplace transform domain

The function $f(r,t)$ is transformed by the Laplace transform with respect to the time t. This transformation is denoted by $\bar{f}(r,s)$ and is defined as follows:

$$\bar{f}(r,s) = \int_0^\infty f(r,t)\, e^{-st} dt. \tag{47}$$

In this context, the complex frequency parameter is denoted by s. Through the utilization of the Laplace transform on the governing equations, it is possible to transform the partial differential equations into the subsequent algebraic and differential equations:

$$(\nabla^2 - s^2)\bar{e} = \nabla^2(\bar{\theta} + \bar{C}), \tag{48}$$

$$\varepsilon\omega_1 \bar{e} = (\nabla^2 - \omega_1)\bar{\theta} - \eta_1 \omega_1 \bar{C}, \tag{49}$$

$$\nabla^2\bar{e} = (\eta_3\,\nabla^2 - \omega_2)\bar{C} - \eta_4\,\nabla^2\bar{\theta}, \tag{50}$$

$$\bar{\sigma}_{rr} = \xi_1\bar{e} + \xi_2\frac{d\bar{u}}{dr} - (\bar{\theta} + \bar{C}), \tag{51}$$

$$\bar{\sigma}_{\Theta\Theta} = \xi_1\bar{e} + \xi_2\frac{\bar{u}}{r} - (\bar{\theta} + \bar{C}), \tag{52}$$

$$P = \eta_3\bar{C} - e - \eta_4\bar{\theta}, \tag{53}$$

where

$$\omega_1 = \frac{s^2\left(1+\tau_0^{\alpha}G(s)\right)}{s+\gamma_1}, \omega_2 = \frac{\eta_2 s^2\left(1+\tau_1^{\alpha}\,G(s)\right)}{s+\gamma_2}, G(s) = \frac{1}{1-\alpha}\frac{\mathrm{s}^{\alpha}}{\mathrm{s}^{\alpha}+\alpha/(1-\alpha)}. \tag{54}$$

It is important to note that the Laplace transform of a fractional differential operator will transform to $G(s) = \mathrm{s}^{\alpha}$ when the fractional differential derivative of Caputo is applied.

In order to eliminate functions $\bar{C}$ and $\bar{e}$, the transformed Laplace equations (48) and (49) can be substituted into Eq (50). This method of deletion yields

$$(\nabla^6 - \Lambda_1\nabla^4 + \Lambda_2\nabla^2 - \Lambda_3)\,\bar{\theta} = 0, \tag{55}$$

where

$$\begin{gathered}\Lambda_1 = \frac{y_3x_1+y_2+y_1x_3-x_2}{y_1-x_1}, \Lambda_2 = \frac{x_2y_3-y_2x_3+y_1x_4}{y_1-x_1}, \Lambda_3 = \frac{x_4y_2}{y_1-x_1},\\ x_1 = \frac{\omega_1(\varepsilon\eta_3+\eta_1)}{\eta_3}, x_2 = \frac{\varepsilon\omega_1\omega_2}{\eta_3}, x_3 = \frac{\omega_2+\eta_3\omega_1+\eta_1\eta_4\omega_1}{\eta_3}, x_4 = \frac{\omega_1\omega_2}{\eta_3},\\ y_1 = \omega_1(\varepsilon+\eta_1), y_2 = s^2\eta_1\omega_1, y_3 = \omega_1(\eta_1-1).\end{gathered} \tag{56}$$

The elimination method can also be applied to obtain the following differential equations

$$(\nabla^6 - \Lambda_1\nabla^4 + \Lambda_2\nabla^2 - \Lambda_3)\;\bar{e} = 0, \tag{57}$$

$$(\nabla^6 - \Lambda_1\nabla^4 + \Lambda_2\nabla^2 - \Lambda_3)\,\bar{C} = 0. \tag{58}$$

The characteristic polynomial of Eq (55) can be written as follows:

$$m^6 - \Lambda_1 m^4 + \Lambda_2 m^2 + \Lambda_3 = 0. \tag{59}$$

When factoring Eq (55), we obtain

$$(\nabla^2 - m_1^2)(\nabla^2 - m_2^2)(\nabla^2 - m_3^2)\,\bar{\theta} = 0. \tag{60}$$

The values of the parameters m_1, $m_2$and m_3 can be determined by solving Eq (59) as follows:

$$\begin{gathered}m_1 = \sqrt{\frac{2p\sin(q)+A_1}{3}}, \qquad m_2 = \sqrt{\frac{A_1-p\left(\sqrt{3}\cos(q)+\sin(q)\right)}{3}},\\ m_3 = \sqrt{\frac{A_1+p\left(\sqrt{3}\cos(q)-\sin(q)\right)}{3}}, \quad p = \sqrt{A_1^2 - 3A_2},\\ q = \frac{1}{3}\sin^{-1}(\chi), \quad \chi = -\frac{1}{2p^3}(2A_1^3 - 9A_1A_2 + 27A_3).\end{gathered} \tag{61}$$

Under the regularity requirement, Eq (60) can be solved and has the following form

$$\bar{\theta}(r,s) = \sum_{i=1}^{3} B_i(s)K_0(m_i r). \tag{62}$$

In this equation, B_i, $i = 1$, 2 and 3 represent the integral parameters, while $K_0(m_i r)$ represents the second sort of Modified Bessel function with a zero order.

Similarly, we can write

$$\bar{e}(r,s) = \sum_{i=1}^{3} B_i'(s)K_0(m_i r), \tag{63}$$

$$\bar{C}(r,s) = \sum_{i=1}^{3} B_i''(s)K_0(m_i r). \tag{64}$$

It is possible to construct the following relations by incorporating Eqs (63) and (64) into Eqs (48) and (49):

$$B_i' = \Gamma_i B_i, \ \ \Gamma_i = \frac{m_i^4 + y_3 m_i^2}{y_1 m_i^2 - y_2}, \ B_i'' = \Omega_i B_i, \ \Omega_i = \frac{m_i^2(1-\Gamma_i) - s^2}{m_i^2}. \tag{65}$$

Then, Eqs (58) and (59) can be represented as follows:

$$\bar{e} = \sum_{i=1}^{3} \Gamma_i B_i K_0(m_i r), \tag{66}$$

$$\bar{C} = \sum_{i=1}^{3} \Omega_i B_i K_0(m_i r). \tag{67}$$

Taking advantage of the relationship between $\bar{u}$ and dilatation $\bar{e}$, the finite solution for the radial displacement $\bar{u}$ can be determined as follows:

$$\bar{u}(r,s) = -\sum_{i=1}^{3} (\Gamma_i/m_i) B_i K_1(m_i r). \tag{68}$$

The thermal stress and chemical potential solutions may be derived by substituting the functions $\bar{\theta}$, $\bar{e}$, $\bar{u}$, and $\bar{C}$ into Eqs (51)–(53):

$$\bar{\sigma}_{rr} = \sum_{i=1}^{3} \big((\Gamma_i - 1 - \Omega_i) K_0(m_i r) + \Gamma_i \xi_2 K_1(m_i r)/(m_i r) \big) B_i, \tag{69}$$

$$\bar{\sigma}_{\Theta\Theta} = \sum_{i=1}^{3} \big((\xi_1 \Gamma_i - 1 - \Omega_i) K_0(m_i r) - \Gamma_i \xi_2 K_1(m_i r)/(m_i r) \big) B_i, \tag{70}$$

$$\bar{P} = \sum_{i=1}^{3} (\eta_3 \Omega_i - \eta_4 - \Gamma_i) K_0(m_i r) B_i. \tag{71}$$

In the transformed domain, the boundary conditions (44)–(46) can be written as follows:

$$\begin{aligned} &\bar{\theta}(r,s) = \frac{4\theta_0(-3+4s+4s^2)}{(5+4s+4s^2)^2} = \bar{M}(s), \qquad \text{at} \quad r = R, \\ &\bar{\sigma}_{rr}(r,s) = 0, \qquad \bar{P}(r,s) = \frac{P_0}{s}, \qquad \text{at} \quad r = R. \end{aligned} \tag{72}$$

By applying the above boundary conditions (72) to the Eqs (62), (70), and (71), we can derive the following system of linear equations:

$$\sum_{i=1}^{3} B_i(s)K_0(m_i R) = \bar{M}(s), \tag{73}$$

$$\sum_{i=1}^{3}\left[(\Gamma_i - 1 - \Omega_i)K_0(m_iR) + \frac{\Gamma_i\xi_2}{m_ir}K_1(m_iR)\right]B_i = 0, \tag{74}$$

$$\sum_{i=1}^{3}(\eta_3\Omega_i - \eta_4 - \Gamma_i)K_0(m_iR)B_i = P_0/s. \tag{75}$$

By solving the system (68)–(70), the values of the integral parameters B_1, B_2, and B_3 can be determined.

7. Generalized MGT model of thermoelasticity without diffusion

The theory of thermoelasticity without diffusion involves making simplified assumptions about the coupled thermal and mechanical processes that occur in an elastic material. In the absence of mass diffusion effects, the functions C and P are eliminated from the basic equations. This enables us to concentrate solely on the interplay between thermal and mechanical behavior in elastic materials. Using the same previous technique, the following two differential equations can be obtained for the functions $\bar{\theta}$ and $\bar{e}$ inside the Laplace transform field:

$$(\nabla^2 - s^2)\bar{e} = \nabla^2\bar{\theta}, \tag{76}$$

$$\varepsilon\omega_1\bar{e} = (\nabla^2 - \omega_1)\bar{\theta}. \tag{77}$$

Additionally, the stress-strain-temperature relations can be expressed as

$$\bar{\sigma}_{rr} = \xi_1\bar{e} + \xi_2\frac{d\bar{u}}{dr} - \bar{\theta}, \tag{78}$$

$$\bar{\sigma}_{\Theta\Theta} = \xi_1\bar{e} + \xi_2\frac{\bar{u}}{r} - \bar{\theta}. \tag{79}$$

In the equations shown above, by removing either $\bar{e}$ or $\bar{\theta}$, the following fourth-order differential equation can be derived:

$$(\nabla^4 - E_1\nabla^2 + E_2)\{\bar{\theta}, \bar{e}\} = 0, \tag{80}$$

where

$$E_1 = s^2 + \omega_1(\varepsilon + 1), E_2 = s^2\omega_1. \tag{89}$$

Equation (80) has a solution that may be expressed as

$$\bar{\theta} = \sum_{i=1}^{2} K_0(n_ir)L_i(s), \tag{90}$$

$$\bar{e} = \sum_{i=1}^{2} H_iK_0(n_ir)L_i(s), \tag{91}$$

where L_i, $i = 1$, and 2 are integral constants. Also, the parameters H_i and n_i^2 are given by

$$H_i = \frac{n_i^2 - \omega_1}{\varepsilon\omega_1},\ n_j^2 = \frac{1}{2}\left(E_1 \pm \sqrt{E_1^2 - 4E_2}\right). \tag{92}$$

The expressions of additional physical fields, including thermal stresses and displacement, can be simplified similarly to the preceding analysis, using the aforementioned solutions:

$$\bar{u} = -\sum_{i=}^{2} \frac{H_i}{m_i} K_1(n_i r) L_i(s), \tag{93}$$

$$\bar{\sigma}_{rr} = \sum_{i=1}^{2} \left[(H_i - 1) K_0(n_i r) + \frac{H_i \xi_2}{m_i r} K_1(n_i r) \right] L_i, \tag{94}$$

$$\bar{\sigma}_{\Theta\Theta} = \sum_{i=1}^{2} \left[(\xi_1 H_i - 1) K_0(n_i r) - \frac{H_i \xi_2}{m_i r} K_1(n_i r) \right] L_i. \tag{95}$$

The boundary conditions in Eqs (44) and (45) may be enough to find the integration constants L_i (where $i = 1$ and 2). This would solve the thermoelasticity problem completely without mass diffusion.

8. Laplace transforms inversion

The Laplace transform is a mathematical method used to convert functions from the time domain to the frequency domain (or complex domain). This transformation frequently facilitates the analysis of differential equations by making them easier to work with. However, to resolve issues in the Laplace domain, the solution must ultimately be converted back to the time domain using an inverse Laplace transform Many people use an approximation algorithm method that uses Fourier series expansion to do inverse Laplace transforms [41] to figure out the numbers of time domain functions from their Laplace-transformed representations. This technique allows us to estimate the inverse Laplace transform using the following formula:

$$g(r,t) = \frac{e^{\varpi t}}{t_{max}} \left(\frac{\bar{g}(r,\varpi)}{2} + Re \sum_{k=1}^{\mathcal{N}} e^{\left(\frac{ik\pi t}{t_{max}}\right)} \bar{g}\left(r, \varpi + \frac{ik\pi}{t_{max}}\right) \right), 0 \le t \le t_{max}. \tag{96}$$

The constant " ϖ " is used to offset the real part of the complex frequency, which guarantees the convergence of the series. t_{max} represents the maximum duration during which we aim to calculate the inverse, and the parameter $\mathcal{N}$ represents the total number of terms in the Fourier series. Increasing the value of $\mathcal{N}$ generally leads to a more accurate approximation, but it also necessitates more computational resources. Specifically, the parameter $\mathcal{N}$ can be determined to satisfy the following relationship:

$$e^{\varpi t} Re\left(e^{\frac{i\mathcal{N}\pi t}{t_{max}}} g(r, \varpi + i\mathcal{N}\pi / t_{max}) \right) \le \mathcal{E}. \tag{97}$$

The parameter $\mathcal{E}$ represents the required threshold for the error or residual in the approximation. If the magnitude of this term is very small, it implies that adding more terms will have a negligible effect, indicating that the approximation is suitably precise. Based on our numerical analysis, we observed that the value of ϖt between 5 and 10 yielded satisfactory outcomes for $\mathcal{N}$ values ranging from 50 to 5000. In our numerical results, we selected a value of $\varpi t = 5$, $t_{max} = 20$, and $\mathcal{N} = 2000$.

9. Numerical example and discussion

Presenting and explaining the numerical results is a powerful way to confirm the success of the

newly proposed model and give a complete picture of how diffusion and some physical phenomena affect the regions studied. Visual images and spreadsheets effectively illustrate the relationship between physical fields and other physical phenomena. We will compare the results obtained with those in the relevant literature. Copper is a versatile metal that exhibits exceptional thermal conductivity, electrical conductivity, and ductility. These features make it widely used in a variety of applications, especially thermoelasticity issues where thermal and mechanical effects are interrelated. This study will demonstrate numerical calculations based on the physical properties of copper which are expressed in international system units as follows [42,43]:

$$T_0 = 293(\mathrm{K}),\ \ \rho = 8954(\mathrm{kg/m^3}),\ \tau_0 = 0.02\mathrm{s}, C_E = 383.1(\mathrm{J/kg\ K}),$$
$$\alpha_t = 1.78 \times 10^{-5}(1/\mathrm{K}),\ \alpha_c = 1.98 \times 10^{-4}(\mathrm{m^3/kg}), R = 1, \tau_1 = 0.2\mathrm{s},$$
$$\{\mu, \lambda\} = \{3.86, 7.76\} \times\ 10^{10}(\mathrm{kg/m\ s^2}), b = 0.9 \times\ 10^{6}(\mathrm{m^5/kg\ s^2}),$$
$$a = 1.2 \times\ 10^{4}(\mathrm{m^2/s^2 K}), K = 386(\mathrm{W/mK}), D = 0.85 \times 10^{-8}(\mathrm{kg\ s/m^3}).$$

For the purpose of calculations, the parameter values $t = 0.12$, $\gamma_1 = 1$ and $\gamma_2 = 0.5$ shall be utilized, unless stated otherwise. To determine the numerical values of the system's physical fields, including temperature change θ, radial displacement u, radial stress σ_{rr}, hoop stress $\sigma_{\Theta\Theta}$ and concentration C as also the chemical potential P, the numerical algorithm described in Eq (96) will be utilized.

9.1. Comparison of different thermal diffusion models

In order to thoroughly analyze the behavior and performance of the proposed heat transfer and fractional mass diffusion models, we will compare the numerical findings obtained with those of earlier models. This comparison will authenticate the precision and dependability of the suggested model. Furthermore, we will perform sensitivity analysis to investigate the impact of various factors on the model predictions. In this part, we'll look at how the MGT fractional thermodiffusion model, the extended fractional thermal diffusion theory with thermal relaxation time (LS-FD), and the classical thermodiffusion theory (CTE-D) compare from one another. Both the theory of fractional thermal diffusion without energy dissipation (GN-II-FD) and the theory of fractional thermodiffusion with energy dissipation (GN-III-FD) will be considered.

The graphical examples presented in Figures 2–8 depict the radial distribution of physical fields. These samples are representative of several thermal diffusion models. By comparing the graphs, we might get a better idea of how different thermal diffusion models affect how temperature, pressure, and other physical properties are spread out in a thermoelastic material with a cylinder-shaped cavity.

Different diffusional thermoelastic models in Figure 2 show the relationship between temperature (θ) and radial distance (r). These models take mass diffusion into account. From the figure, it can be observed that the temperature values reach their highest point at the surface of the spherical cavity ($r = 1$) due to the presence of a dynamic thermal field at the surface. This result indicates that the problem's thermal boundary condition is satisfied by the temperature distribution. As the radius direction (r) increases, the temperature drops and continues to move in the opposite direction of heat wave propagation. Gradually, it diminishes until the temperature hits zero. This indicates that the transport of heat within the flexible medium occurs at restricted velocities, in accordance with empirical data. Efficient electronic component performance relies on critical heat management to

prevent overheating. The progressive decline in temperature with increasing radial distance signifies the need for heat sinks and cooling systems to be engineered to accommodate the finite rate of heat transmission. A comparison of the qualitative results with the relevant literature reveals that the findings of other authors, such as those in [44,45], are consistent with the current behavior of the qualitative data.

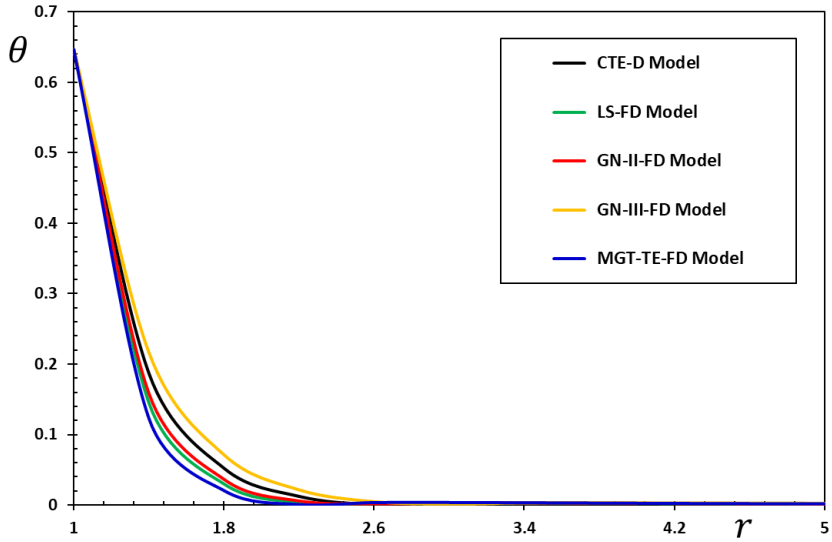

Figure 2. Temperature change θ under thermal diffusion models.

Efficient thermal management is important in order to avoid excessive heat buildup, which can result in decreased performance, component malfunctions, and a shortened system lifespan. Through the examination of heat dissipation and distribution in different operational scenarios, engineers can develop more effective cooling methods and enhance system performance and durability [46]. Furthermore, precise thermal modeling can assist in anticipating potential thermal problems in advance, allowing proactive steps to be implemented to avert any detrimental impacts on the system [47].

Temperature fluctuations (θ) in a substance can result in thermal expansion or contraction, which subsequently induces displacement inside the substance. The occurrence is referred to as thermal strain. The displacement u can lead to the formation of thermal stresses, which can greatly impact the structural integrity of a material or component. Figure 3 examines the impact of various parameters, such as relaxation times, on the behavior of the displacement distribution (u) produced by several thermal diffusion models. The figure indicates that the radial displacement distribution (u) starts with a negative value and increases rapidly, peaking around the point $r = 1.6$, then gradually decreases again to zero with increasing distance from the center of the cylindrical cavity. The shape curves also indicate that the thermal relaxation times τ_0 and diffusive relaxation times τ_1 play a crucial role in the body's deformation behavior.

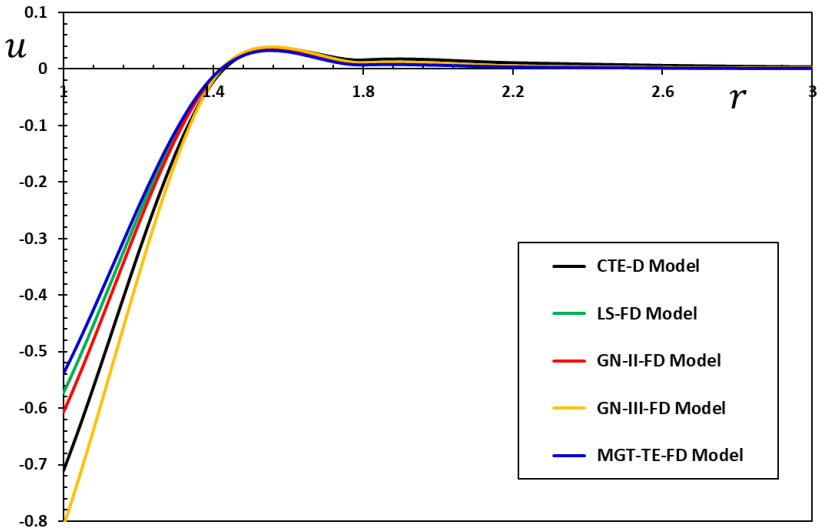

Figure 3. Radial displacement u under thermal diffusion models.

Figures 4 and 5 are presented for the purpose of comparing the impact of various thermodiffusion models on the variability of thermal stresses (σ_{rr} and $\sigma_{\Theta\Theta}$). These visual representations allow for the examination of stress fluctuations and model comparisons. Figure 4 demonstrates that the radial thermal stress σ_{rr} begins at zero, signifying the fulfillment of the imposed mechanical boundary conditions and the accuracy of the numerical findings. The value rises rapidly to reach a maximum, which could indicate the thermal stress resulting from the diffusion and expansion of heat in the radial direction. The magnitude of the radial stress σ_{rr} increases rapidly until it reaches its maximum value at $r = 1.6$, after which it gradually diminishes until it approaches zero. This behavior is consistent with the usual thermal stress patterns, in which tension accumulates as a result of thermal expansion and then decreases as heat spreads and the material reaches a state of balance. Understanding these patterns is essential to ensure the structural integrity of spherical cavities and other geometries subjected to thermal stresses. This aligns with the findings acquired by Geetanjali and Sharma [48].

Figure 5 illustrates that the hoop stress $\sigma_{\Theta\Theta}$ initially has a negative value, indicating the presence of compressive stress on the surface of the spherical cavity. This is consistent with the hoop stress's fatigue characteristics, where the interior structure may experience stress as a result of expansion and heat deformation. The hoop stress $\sigma_{\Theta\Theta}$ has a similar pattern to σ_{rr}, characterized by a quick ascent to a maximum value followed by a steady decline to zero. According to its inherent characteristics, thermal stress causes compression in the outer layers and expansion in the inner layers, resulting in an equilibrium between radial and hoop loads. The diffusion thermoelasticity models LS-FD, GN-II-FD, and MGT-TE-FD display a low trend compared to other models. This suggests that these models may have common assumptions or formulas in their approach to thermal elasticity and diffusion.

Figure 6 visually represents the numerical calculations of the chemical potential P as a function of the radial distance r for the five different thermodiffusion models. Figure 6 illustrates that initially, the chemical potential P exhibits a high variance, but the transition vibrations gradually diminish and become less noticeable with increasing r value. We have successfully determined the chemical potential P profile by initially considering the highest surface value and ensuring that it satisfies the imposed boundary constraints. In agreement with the boundary conditions of the issue, it can be

observed that the chemical potential with maximal values $P = 1$ is found at the surface $r = 1$. This process has confirmed and validated our results. We conducted a comparative analysis of five theories, namely CTE-D, LS-FD, GN-II-FD, GN-III-FD, and MGT-TE-FD, for thermoelastic diffusion. We observed that the variations in the coupled thermal diffusion state and GN-III-FD are comparable to each other and exhibit the greatest amounts. However, the LS-FD models, GN-II-FD, and MGT-TE-FD exhibit smaller magnitudes, likely due to the influence of extended thermal relaxation factors. The results of Figure 6 reveal that the proposed model (MGT-TE-FD), which includes the relaxation coefficients of generalized thermoelasticity and diffusion, significantly influences the properties and behavior of the chemical potential distribution (P).

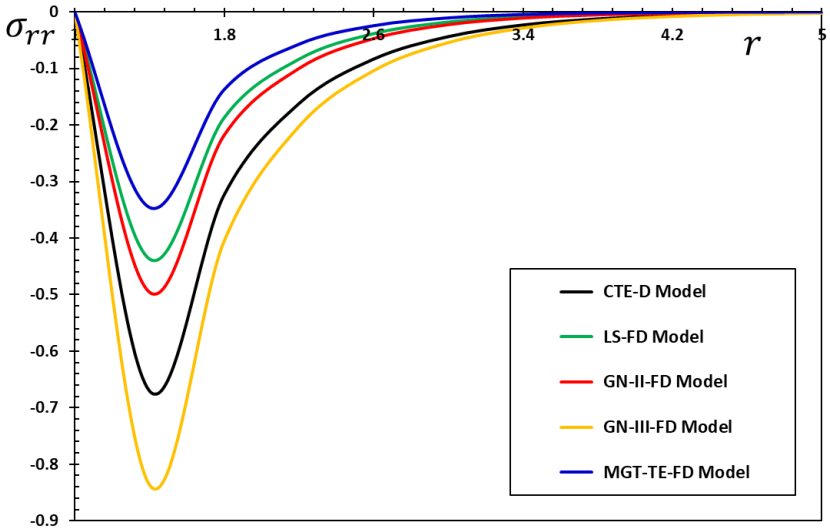

Figure 4. Thermal stress σ_{rr} under thermal diffusion models.

Relaxation times (τ_0 and τ_1) are essential in mass thermoelastic diffusion models since they determine the mass concentration distribution (C) within an elastic medium. These relaxation times correspond to the specific timescale at which the system achieves a new equilibrium state in reaction to alterations in mass concentration or other thermodynamic variables. Figure 7 illustrates how the presence of relaxation durations affects the concentration distribution in an infinite elastic media according to the mass thermoelastic diffusion models. The data in Figure 7 indicates that the mass concentration values increase as the initial distance r values increase until they reach a maximum point, following which they gradually decrease within the thermoelastic medium. This indicates a decrease in concentration levels within the thermoelastic material. As the mass concentration declines following the peak, it signifies that the diffusion process has reached a stage where the substance is being more uniformly dispersed or starting to disperse. The correlation between mass concentration and thermal stress in thermoelastic mediums is of utmost importance. Variations in mass concentration can impact mechanical qualities, resulting in changes in thermal stress. When mass diffusion affects the mechanical properties of materials, as in industrial operations or material creation, a thorough understanding of this concept is essential.

These relaxation times (τ_0 and τ_1) likely influenced the dissipation of thermal waves. The CTE-D and GN-III-D thermoelastic-diffusion models exhibited elevated temperature values in comparison

to the GN-II-D, LS-D, and MGT-TE-D thermodiffusion models. These findings indicate that the CTE-D and GN-III-D models result in reduced dissipation of thermal waves, resulting in elevated temperatures [49]. The fractional MGT-TE-D thermodiffusion model accurately predicted a significant decline in temperature, which can be attributed to the inclusion of relaxation times (τ_0 and τ_1) in the derived equations [50].

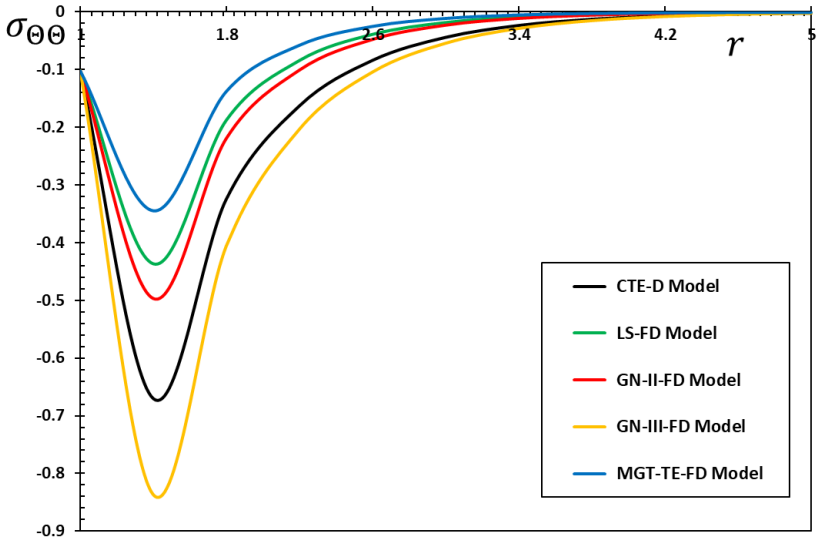

Figure 5. Thermal stress $\sigma_{\Theta\Theta}$ under thermal diffusion models.

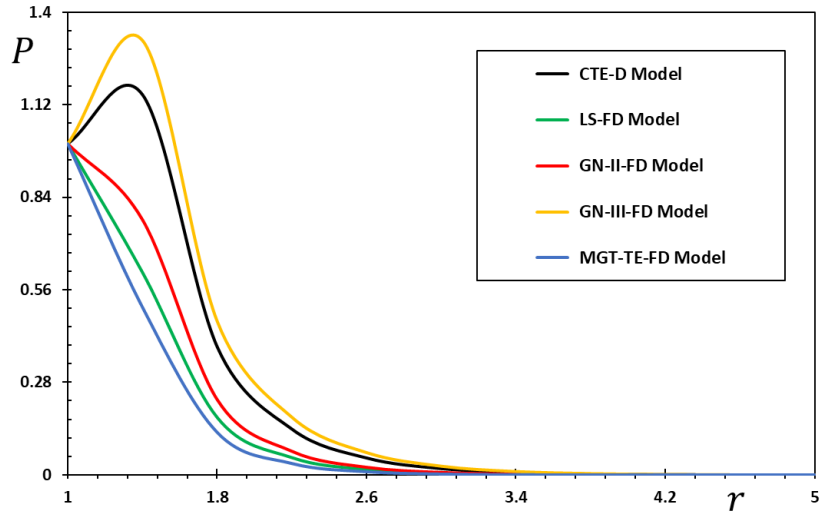

Figure 6. Chemical potential P under thermal diffusion models.

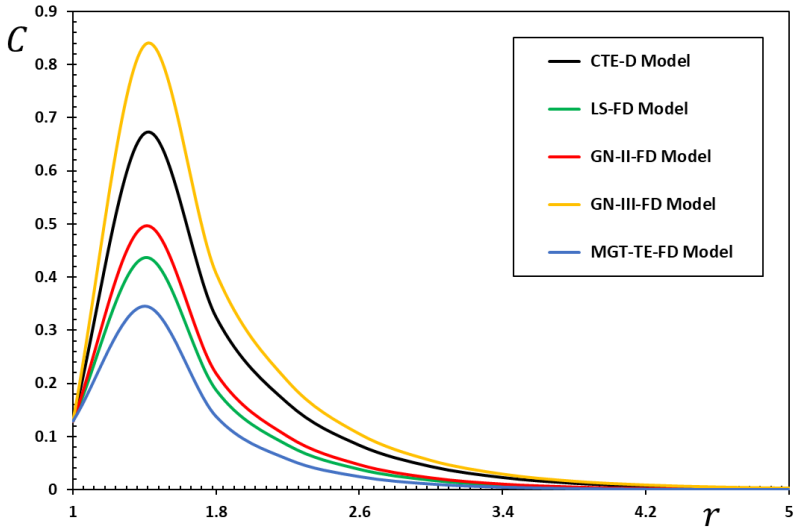

Figure 7. Mass concentration C for different thermal diffusion models.

The present thermoelastic-diffusion model incorporates the interplay of thermal, mechanical, and diffusive phenomena in the material. This model provides a more thorough understanding of heat transfer processes by considering the finite pace at which heat spreads as well as the interplay between heat, stress, and mass diffusion within the material. The thermoelastic-diffusion model provides a more precise depiction of heat transport phenomena in real-world situations by including extra parameters such as fractional operators and relaxation time. This aligns with the empirical observations and validates the significance of the suggested model, which is in line with the findings given in [51,52].

Engineers can enhance the durability of structures by comprehending the relationship between temperature variations, displacement, and thermal stresses. Additionally, taking into account the finite pace at which heat spreads enables the design of structures that can better endure thermal cycling and uphold their structural integrity in the long run.

9.2. Effects of fractional differential derivatives

Thermoelastic models are affected by nonlocal influences when fractional differential derivatives are introduced. Unlike traditional derivatives that only evaluate the current state of a system, fractional derivatives account for the entire history of the system over a specific time or space. This phenomenon of nonlocal behavior captures long-range interactions and memory effects in matter interaction. Thermoelastic models can exhibit anomalous diffusion behavior as a result of fractional derivatives. Anomalous diffusion pertains to scenarios where the propagation of heat or mass deviates from the predictions of classical diffusion equations. Fractional derivatives enable the characterization of sub-diffusion (slower than classical diffusion) or super-diffusion (faster than classical diffusion) processes. Integrating fractional differential derivatives into thermoelastic models may enhance accuracy in representing the behavior of actual materials in certain instances. Fractional derivatives provide a versatile and sophisticated mathematical framework that can more accurately depict intricate processes and empirical phenomena.

This subsection of the discussion and analysis will examine the particular consequences and ramifications of incorporating fractional differential derivatives into diffusional thermoelastic models.

Additionally, the behavior of the physical fields of the system will be influenced by varying the order of the fractional derivatives employed. Only the MGT fractional thermal diffusion (MGT-TE-FD) model will be considered. This study will compare traditional integer-order differential actuators with fractional actuators with memory effects, notably those utilizing Caputo (C) and Atangana-Baleanu (AB) fractional derivatives. The AB fractional derivative is a distinct fractional derivative operator that has garnered significant interest in recent times. It offers an alternative mathematical expression in contrast to the C derivative. The AB fractional derivative utilizes a Mittag-Leffler kernel, which is both nonlocal and non-singular in nature.

Figures 8–13 illustrate the response of many physical parameters, including temperature θ, chemical potential P, radial displacement u, thermal pressures (σ_{rr} and $\sigma_{\Theta\Theta}$), and mass concentration C, under the condition of constant thermal diffusion relaxation times (τ_0 and τ_1). The data presented in Figures 8 and 9 demonstrate that reducing the fractional order parameter (α) from 1.00 to 0.70 results in a deceleration in thermal diffusion wave propagation. Moreover, the magnitude of the chemical potential diminishes as α decreases near the wavefront. Figure 10 indicates that decreasing the value of α from 1.00 to 0.60 results in a greater degree of thermal displacement u. Additionally, it has been demonstrated that the elastic wavefront exhibits retrograde motion, which suggests a reduced velocity of the elastic wave. Figures 11 and 12 demonstrate that as the value of α decreases, there is a significant improvement in the peak value of thermal stresses and enlargement of the stress response region. Figure 13 shows that before the arrival of the heat wave, the magnitude of the concentration variation (C) was steadily decreasing as the fractional order (α) decreased. It is clear from this discussion that fraction-order must be added to the constitutive relations of generalized thermoelastic diffusion theory because it has such a huge effect on the transient responses of structures.

The figures clearly demonstrate that incorporating fractional differential derivatives into thermoelastic models allows for the representation of more intricate and realistic phenomena, such as anomalous diffusion and memory effects. This, in turn, enhances the accuracy of modeling and deepens our understanding of the underlying physical processes. This phenomenon aligns with the findings mentioned in reference [53].

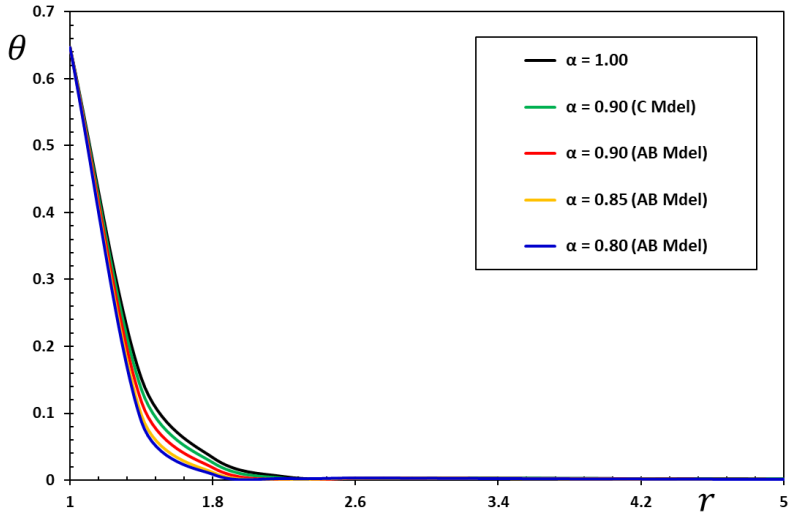

Figure 8. Temperature change θ under different fractional operators and fractional order parameter.

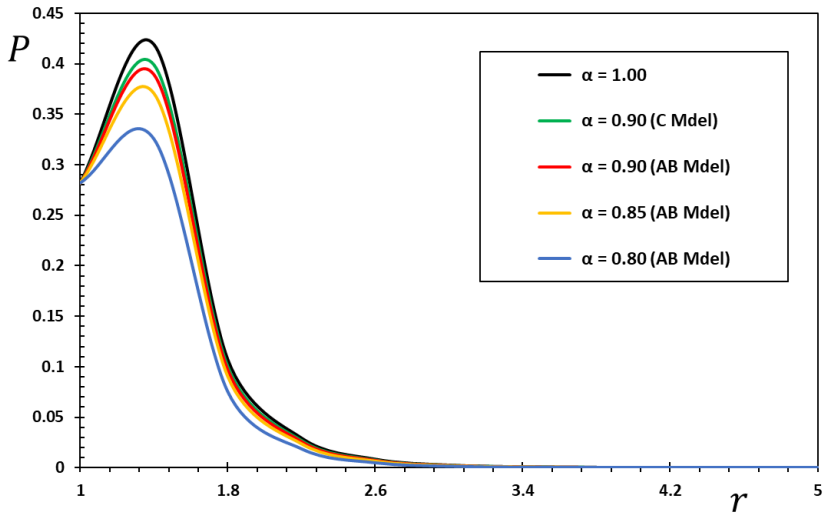

Figure 9. The chemical potential P under different fractional operators and fractional order parameter.

The various graphs demonstrate that the differential operator selection, such as the C or AB fractional derivative, significantly influences the mathematical formulation and operation of the fractional model. Varied interpretations of fractional derivatives can result in different characteristics and solutions for wave equations and physical fields within a given system. In addition to this, it is observed that the magnitude of the partial order parameter has a significant impact on the stability and equilibrium conditions of waves [54]. Specific ranges of fractional orders might result in steady wave propagation, while other ranges may cause instability or oscillatory behavior.

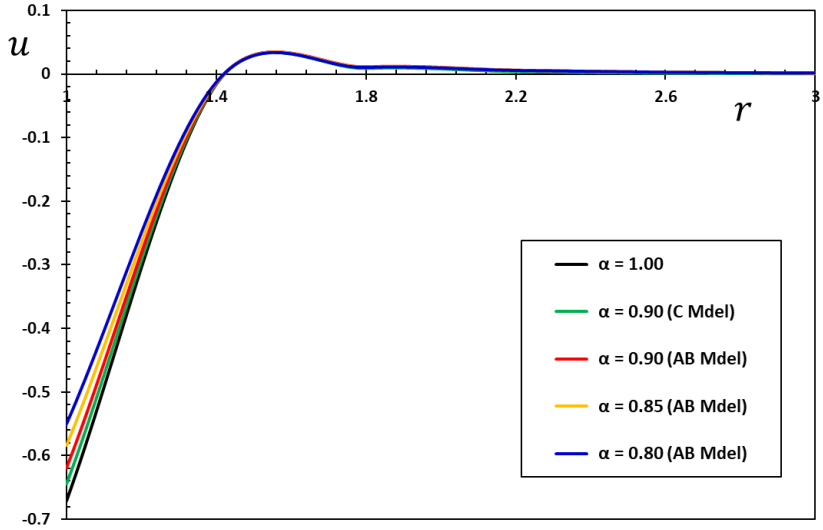

Figure 10. The radial displacement u under different fractional operators and fractional order parameter.

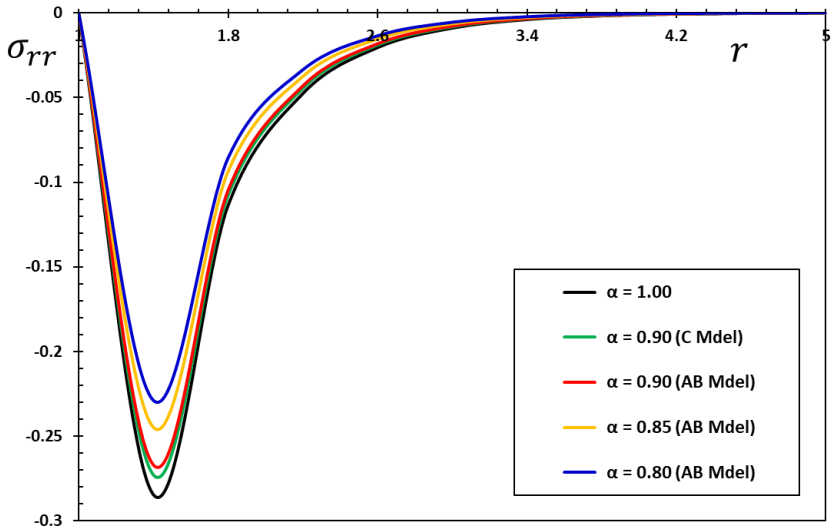

Figure 11. The radial stress σ_{rr} under different fractional operators and fractional order parameter.

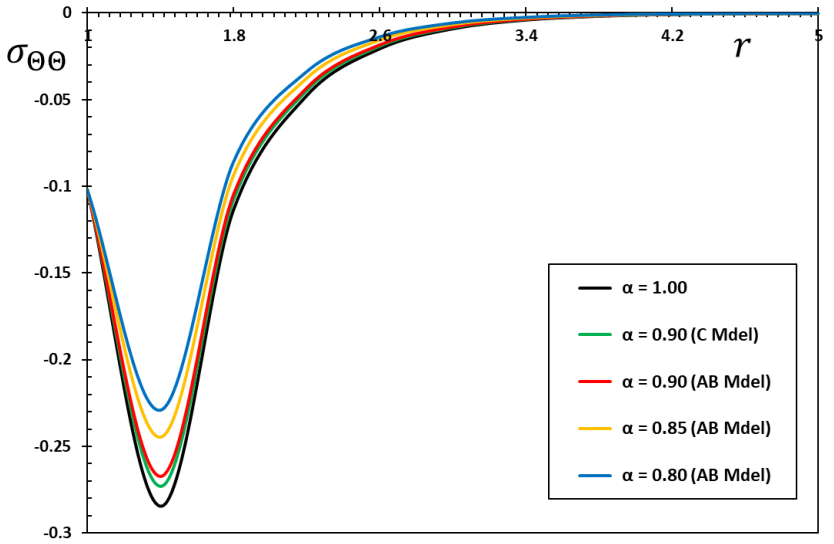

Figure 12. The hoop stress $\sigma_{\Theta\Theta}$ under different fractional operators and fractional order parameter.

The comparison of the results demonstrates the efficacy of the study and the present fractional model in aligning with the findings of earlier scholarly works, as referenced in [55]. The temperature distribution and thermal stress exhibit a strong correlation with variations in the fractional operator. This suggests that the numerical approach and methods employed in this study are precise and efficient. Also, it was shown that the AB operator slows down the propagation of thermomechanical waves compared to other operators. This suggests that the unique properties of this fractional operator help to improve attenuation and damping. This behavior has important effects on thermoelastic modeling because it shows how important memory effects, nonlocality, and larger interactions are for getting

stable and reliable solutions [56]. The choice of a fractional operator can have a significant impact on the characteristics of thermoelastic systems, making the AB operator a valuable asset in situations where wave attenuation and control are critical.

After analyzing the curves and comparing various forms of fractional operators, it can be concluded that the AB operator outperforms the C operator significantly and the conventional differential derivative in modeling diffusive heat conduction in thermoelastic media. The non-singular and nonlocal kernel of the AB operator, due to its use of the Mittag-Leffler function, along with its versatility and wider scope of use, makes it a potent instrument for simulating intricate thermoelastic systems. The behavior of the present results shows good agreement with [57]. This advantage can result in more precise and dependable forecasts in engineering and scientific scenarios where diffusive heat conduction is critical.

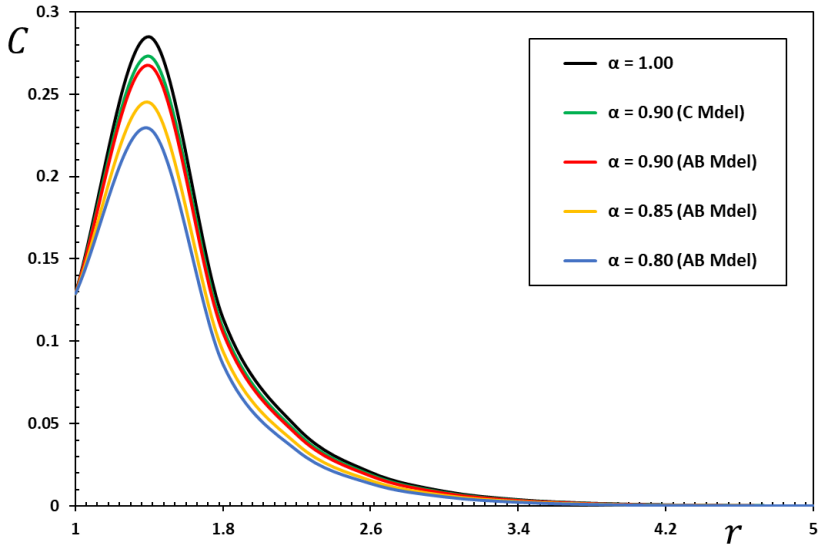

Figure 13. The mass concentration C under different fractional operators and fractional order parameter.

Finally, the graphs emphasize the importance of choosing the correct fractional derivative operator for a specific problem in order to precisely simulate and examine fractional systems' behavior. Understanding the effects of distinct derivative operators on fractional equation solutions is critical for achieving dependable and significant outcomes in a variety of scientific and engineering applications. Reduced wave propagation is beneficial for the development of materials and structures that may experience problems due to excessive thermomechanical waves, such as microelectronics, precision instruments, or heavy loads. The high damping and attenuation of the AB actuator demonstrate its ability to model systems that require wave control and reduction.

10. Conclusions

The current study introduces a novel fractional thermoelastic diffusion model that integrates the AB fractional operator. The AB fractional derivative utilizes a Mittag-Leffler kernel, which is nonlocal and nonsingular. The development of the novel fractional thermoelastic diffusion model focuses on the MGT equation. Compared to the C derivative, which may exhibit singularities, the AB operator's

Mittag-Leffler kernel offers a more stable and adaptable formulation. Additionally, the nonsingular nature of this function improves stability and convergence in mathematical formulations. The constitutive equations, as well as the heat and mass diffusion equations, have been adjusted to include the AB fractional operator. The introduction of this novel fractional model aims to resolve the perceived discrepancy between the infinite thermal and diffusion rates predicted by conventional theories of thermoelastic diffusion and the energy dissipation model proposed by Green and Naghdi (GN-III).

Analysis of the results allows the following final conclusions to be drawn:

• The novel fractional thermal diffusion model incorporates the MGT equation to include the finite speed of propagation, thus overcoming the constraints of traditional models that assume infinite wave propagation rates.

• The behavior and decay characteristics of thermal and mechanical wave propagation, mass diffusion, and concentration are all affected by delay times in a big way. These parameters slow down the propagation rate of heat waves, influencing their distribution and diminishment within the system.

• The new fractional model of diffusional thermoelasticity incorporates the heat and mass diffusion equations through the fractional differential operator AB. This inclusion enables the consideration of memory and nonlocal effects, resulting in a more realistic representation of behavior and theoretical outcomes that align with observed physical phenomena.

• Fractional differential derivatives offer a potent means of expanding and broadening thermoelastic models. They provide a method to include memory effects, nonlocality, and complicated interactions, hence improving the capability to describe and analyze thermoelastic systems. Although there are difficulties in calculation, fractional derivatives can create models that are more precise and adaptable.

The fractional MGTED model allows for the study of heat and mass transfer processes in porous materials, such as fuel cells, filtration systems, and geothermal reservoirs. Considering the interplay between fluid flow, heat transfer, and mass transport inside porous media, it offers a framework for examining the combined impacts of thermal and diffusion processes. The MGTED model can characterize the thermal behavior and diffusion of advanced materials, including polymers, composites, and nanostructured materials. It facilitates the design and development of materials with tailored thermal and mass transfer characteristics, higher energy efficiency, and better performance in applications such as sensors, membranes, and insulation. Furthermore, the MGTED model allows for the analysis of heat and mass transfer processes in biological tissues and biomaterials. It enables the study of tissue engineering applications, drug delivery systems, and thermal treatment temperature and concentration distributions in tissues. Delay times affect concentration, and the behavior and decay characteristics of mass diffusion, as well as thermomechanical wave propagation. These characteristics influence the spatial distribution and decay of heat waves traveling in the system, thereby slowing down their propagation speed.

Author contributions

Yazeed Alhassan: Conceptualization, Methodology, Formal Analysis, Writing – Original Draft Preparation; Mohammed Alsubhi: Investigation, Data Curation, Visualization, Writing – Review & Editing; Ahmed E. Abouelregal: Supervision, Project Administration, Funding Acquisition, Writing – Review & Editing. All authors have read and agreed to the published version of the manuscript.

Use of AI tools declaration

The authors declare they have not used Artificial Intelligence (AI) tools in the creation of this article.

Acknowledgments

This work was funded by the Deanship of Scientific Research at Jouf University through the Fast-track Research Funding Program

Conflict of interest

The authors declare that they have no competing financial interests or personal relationships.

References

1. I. N. Sneddon, *The linear theory of thermoelasticity*, Wien CISM Udine: Springer-Verlag, 1974.
2. W. A. Day, *Heat conduction within linear thermoelasticity*, Springer, 2013.
3. J. Ba, T. Han, L. Fu, Z. Wang, Review of thermoelasticity theory in rocks and its applications in geophysics, *Rev. Geoph. Planet. Phys*., **52** (2021), 623–633. https://doi.org/10.19975/j.dqyxx.2021-009
4. V. D. Kupradze, *Three-dimensional problems of elasticity and thermoelasticity*, Elsevier, 2012.
5. M. A. Biot, Thermoelasticity and irreversible thermodynamics, *J. Appl. Phys*., **27** (1956), 240–253. https://doi.org/10.1063/1.1722351
6. H. W. Lord, Y. Shulman, A generalized dynamical theory of thermoelasticity, *J. Mech. Phys. Solids*, **15** (1967), 299–309. https://doi.org/10.1016/0022-5096(67)90024-5
7. A. E. Green, K. Lindsay, Thermoelasticity, *J. Elasticity*, **2** (1972), 1–7. https://doi.org/10.1007/BF00045689
8. A. E. Green, P. Naghdi, A re-examination of the basic postulates of thermomechanics, *Proc. Roy. Soc. A Math. Phys. Sci.,* **432** (1991), 171–194. https://doi.org/10.1098/rspa.1991.0012
9. A. E. Green, P. Naghdi, On undamped heat waves in an elastic solid, *J. Therm. Stress*., **15** (1992), 253–264. https://doi.org/10.1080/01495739208946136
10. A. E. Green, P. Naghdi, Thermoelasticity without energy dissipation, *J. Elasticity*, **31** (1993), 189–208. https://doi.org/10.1007/BF00044969
11. F. Dell'Oro, I. Lasiecka, V. Pata, A note on the Moore-Gibson-Thompson equation with memory of type II, *J. Evol. Equ*., **20** (2020), 1251–1268. https://doi.org/10.1007/s00028-019-00554-0
12. R. Quintanilla, Moore-Gibson-Thompson thermoelasticity, *Math. Mech. Solids*, **24** (2019), 4020–4031. https://doi.org/10.1177/1081286519862007
13. R. Quintanilla, Moore-Gibson-Thompson thermoelasticity with two temperatures, *Appl. Eng. Sci*., **1** (2020), 100006. https://doi.org/10.1016/j.apples.2020.100006
14. N. Bazarra, J. R. Fernández, R. Quintanilla, Analysis of a Moore-Gibson-Thompson thermoelastic problem, *J. Comput. Appl Math.*, **382** (2021), 113058. https://doi.org/10.1016/j.cam.2020.113058

15. A. E. Abouelregal, M. Marin, H. Altenbach, Thermally stressed thermoelectric microbeam supported by Winkler foundation via the modified Moore-Gibson-Thompson thermoelasticity theory, *Z. Angew. J. Appl. Math. Mech*., **103** (2023), e202300079. https://doi.org/10.1002/zamm.202300079
16. S. Gupta, S. Das, R. Dutta, Peltier and Seebeck effects on a nonlocal couple stress double porous thermoelastic diffusive material under memory-dependent Moore-Gibson-Thompson theory, *Mech. Adv. Mat. Struct*., **30** (2023), 449–472. https://doi.org/10.1080/15376494.2021.2017525
17. A. E. Abouelregal, M. A. Fahmy, Generalized Moore-Gibson-Thompson thermoelastic fractional derivative model without singular kernels for an infinite orthotropic thermoelastic body with temperature-dependent properties, *Z. Angew. J. Appl. Math. Mech.*, **102** (2022), e202100533. https://doi.org/10.1002/zamm.202100533
18. R. V. Singh, S. Mukhopadhyay, Study of wave propagation in an infinite solid due to a line heat source under Moore-Gibson-Thompson thermoelasticity, *Acta Mech*., **232** (2021), 4747–4760. https://doi.org/10.1007/s00707-021-03073-7
19. L. Sun, Q. Zhang, Z. Chen, X. Wei, A singular boundary method for transient coupled dynamic thermoelastic analysis, *Comput. Math. Appl*., **158** (2024), 259–274. https://doi.org/10.1016/j.camwa.2024.02.017
20. S. A. Davydov, A. V. Zemskov, Thermoelastic diffusion phase-lag model for a layer with internal heat and mass sources, *Int. J. Heat Mass Trans*., **183** (2022), 122213. https://doi.org/10.1016/j.ijheatmasstransfer.2021.122213
21. A. E. Abouelregal, H. M. Sedighi, A new insight into the interaction of thermoelasticity with mass diffusion for a half-space in the context of Moore-Gibson-Thompson thermodiffusion theory, *Appl. Phys. A*, **127** (2021), 582. https://doi.org/10.1007/s00339-021-04725-0
22. A. R. Allnatt, A. V. Chadwick, Thermal diffusion in crystalline solids, *Chem. Rev*., **67** (1967), 681–705. https://doi.org/10.1021/cr60250a005
23. Y. Abebe, T. Birhanu, L. Demeyu, M. Taye, M. Bekele, Y. Bassie, Thermally activated diffusion of impurities along a semiconductor layer, *Eur. Phys. J. B*, **95** (2022), 9. https://doi.org/10.1140/epjb/s10051-021-00265-x
24. J. T. Bauer, X. Montero, M. C. Galetz, Fast heat treatment methods for al slurry diffusion coatings on alloy 800 prepared in air, *Surf. Coat. Technol*., **381** (2020), 125140. https://doi.org/10.1016/j.surfcoat.2019.125140
25. W. Nowacki, Dynamic problems of diffusion in solids, *Eng. Fract. Mech*., **8** (1976), 261–266. https://doi.org/10.1016/0013-7944(76)90091-6
26. H. H. Sherief, F. A. Hamza, H. A. Saleh, The theory of generalized thermoelastic diffusion, *Int. J. Eng. Sci*., **42** (2004), 591–608. https://doi.org/10.1016/j.ijengsci.2003.05.001
27. C. Cattaneo, Sur une forme de l'equation de la chaleur eliminant la paradoxe d'une propagation instantantee, *Compt. Rend*., **247** (1958), 431–433.
28. P. Vernotte, Les paradoxes de la theorie continue de l'equation de la chaleur, *Compt. Rend*., **246** (1958), 3154.
29. A. E. Abouelregal, Generalized mathematical novel model of thermoelastic diffusion with four phase lags and higher-order time derivative, *Eur. Phys. J. Plus*, **135** (2020), 263. https://doi.org/10.1140/epjp/s13360-020-00282-2

30. N. A. Shah, I. Ahmad, O. Bazighifan, A. E. Abouelregal, H. Ahmad, Multistage optimal homotopy asymptotic method for the nonlinear Riccati ordinary differential equation in nonlinear physics, *Appl. Math*., **14** (2020), 1009–1016. http://dx.doi.org/10.18576/amis/140608
31. A. E. Abouelregal, H. Ahmad, A. M. Yahya, A. Saidi, H. Alfadil, Generalized thermoelastic responses in an infinite solid cylinder under the thermoelastic-diffusion model with four lags, *Chin. J. Phys*., **76** (2022), 121–134. https://doi.org/10.1016/j.cjph.2021.08.015
32. N. Sene, A. N. Fall, Homotopy perturbation ρ-Laplace transform method and its application to the fractional diffusion equation and the fractional diffusion-reaction equation, *Fractal Fract.*, **3** (2019), 14. https://doi.org/10.3390/fractalfract3020014
33. J. Hristov, Approximate solutions to fractional subdiffusion equations, *Euro. Phys. J. Spec. Top*., **193** (2011), 229–243. https://doi.org/10.1140/epjst/e2011-01394-2
34. M. M. Meerschaert, C. Tadjeran, Finite difference approximations for fractional advection-dispersion flow equations, *J. Comp. Appl. Math*., **172** (2004), 65–77. https://doi.org/10.1016/j.cam.2004.01.033
35. M. Caputo, Linear models of dissipation whose Q is almost frequency independent—II, *Geophys. J. Int.*, **13** (1967), 529–539. https://doi.org/10.1111/j.1365-246X.1967.tb02303.x
36. A. Atangana, D. Baleanu, New fractional derivatives with nonlocal and non-singular kernel: Theory and application to heat transfer model, *Therm. Sci*., **20** (2016), 763–769. https://doi.org/10.2298/TSCI160111018A
37. A. Atangana, D. Baleanu, Caputo-Fabrizio derivative applied to groundwater flow within confined aquifer, *J. Eng. Mech*., **143** (2017), D4016005. https://doi.org/10.1061/(ASCE)EM.1943-7889.0001091
38. A. Atangana, I. Koca, Chaos in a simple nonlinear system with Atangana-Baleanu derivatives with fractional order, *Chaos Soliton Fract*., **89** (2016), 447–454. https://doi.org/10.1016/j.chaos.2016.02.012
39. M. Caputo, M. Fabrizio, On the notion of fractional derivative and applications to the hysteresis phenomena, *Meccanica*, **52** (2017), 3043–3052. https://doi.org/10.1007/s11012-017-0652-y
40. T. M. Atanacković, S. Pilipović, D. Zorica, Properties of the Caputo-Fabrizio fractional derivative and its distributional settings, *Frac. Calc. Appl. Anal*., **21** (2018), 29–44. https://doi.org/10.1515/fca-2018-0003
41. G. Honig, U. Hirdes, A method for the numerical inversion of Laplace transforms, *J. Comput. Appl. Math*., **10** (1984), 113–132. https://doi.org/10.1016/0377-0427(84)90075-X
42. K. Singh, I. Kaur, E. M. Craciun, Hygro-photo-thermoelastic solid cylinder under moisture and thermal diffusivity with Moore-Gibson-Thompson theory, *Discover Mech. Eng*., **2** (2023), 21. https://doi.org/10.1007/s44245-023-00028-1
43. D. K. Sharma, D. Thakur, Effect of three phase lag model on the free vibration analysis of nonlocal elastic generalized thermo-diffusive sphere, *Mat. Today Proc*., **42** (2021), 370–376. https://doi.org/10.1016/j.matpr.2020.09.560
44. Y. Guo, C. Xiong, L. Wang, K. Yu, Dynamic response of the fractional order thermoelastic diffusion problem of an infinite body with a cylindrical tunnel cavity under different shock loads, *Waves Rand. Comp. Media*, 2022, 1–21. https://doi.org/10.1080/17455030.2022.2099596
45. R. Kumar, N. Sharma, S. Chopra, Photothermoelastic interactions under Moore-Gibson-Thompson thermoelasticity, *Coupled Syst. Mech*., **11** (2022), 459. https://doi.org/10.12989/csm.2022.11.5.459

46. Q. L. Yue, C. X. He, M. C. Wu, T. S. Zhao, Advances in thermal management systems for next-generation power batteries, *Int. J. Heat Mass Trans.*, **181** (2021), 121853. https://doi.org/10.1016/j.ijheatmasstransfer.2021.121853
47. Y. Huang, X. Xiao, H. Kang, J. Lv, R. Zeng, J. Shen, Thermal management of polymer electrolyte membrane fuel cells: A critical review of heat transfer mechanisms, cooling approaches, and advanced cooling techniques analysis, *Energy Conv. Manag.*, **254** (2022), 115221. https://doi.org/10.1016/j.enconman.2022.115221
48. G. Geetanjali, P. K. Sharma, Impact of fractional strain on medium containing spherical cavity in the framework of generalized thermoviscoelastic diffusion, *J. Therm. Stress.*, **46** (2023), 333–350. https://doi.org/10.1080/01495739.2023.2176386
49. S. Gupta, R. Dutta, S. Das, Memory response in a nonlocal micropolar double porous thermoelastic medium with variable conductivity under Moore-Gibson-Thompson thermoelasticity theory, *J. Ocean Eng. Sci.*, **8** (2023), 263–277. https://doi.org/10.1016/j.joes.2022.01.010
50. A. E. Abouelregal, M. Marin, A. Foul, S. S. Askar, Thermomagnetic responses of a thermoelastic medium containing a spherical hole exposed to a timed laser pulse heat source, *Case Stud. Therm. Eng.*, **56** (2024), 104288. https://doi.org/10.1016/j.csite.2024.104288
51. Z. N. Xue, Y. J. Yu, X. G. Tian, Transient responses of multi-layered structures with interfacial conditions in the generalized thermoelastic diffusion theory, *Int. J. Mech. Sci.*, **131** (2017), 63–74. https://doi.org/10.1016/j.ijmecsci.2017.05.054
52. C. Li, H. Guo, X. Tian, Transient responses of a hollow cylinder under thermal and chemical shock based on generalized diffusion-thermoelasticity with memory-dependent derivative, *J. Therm. Stress.*, **42** (2019), 313–331. https://doi.org/10.1080/01495739.2018.1486689
53. A. E. Abouelregal, M. Marin, A. Foul, S. S. Askar, Coupled responses of thermomechanical waves in functionally graded viscoelastic nanobeams via thermoelastic heat conduction model including Atangana-Baleanu fractional derivative, *Sci. Rep.*, **14** (2024), 9122. https://doi.org/10.1038/s41598-024-58866-2
54. W. Gao, P. Veeresha, D. G. Prakasha, B. Senel, H. M. Baskonus, Iterative method applied to the fractional nonlinear systems arising in thermoelasticity with Mittag-Leffler kernel, *Fractals*, **28** (2020), 2040040. https://doi.org/10.1142/S0218348X2040040X
55. A. Genovese, F. Farroni, A.Sakhnevych, Fractional calculus approach to reproduce material viscoelastic behavior, including the time–temperature superposition phenomenon, *Polymers*, **14** (2022), 4412. https://doi.org/10.3390/polym14204412
56. Y. Lu, C. Li, T. He, Fractional-order non-Fick mechanical-diffusion coupling model based on new fractional derivatives and structural transient dynamic responses of multilayered composite laminates, *Arch. Appl. Mech.*, **94** (2024), 239–259. https://doi.org/10.1007/s00419-023-02518-w
57. A. E. Abouelregal, F. Alsharif, H. Althagafi, Y. Alhassan, Fractional heat transfer DPL model incorporating an exponential Rabotnov kernel to study an infinite solid with a spherical cavity, *AIMS Mathematics*, **9** (2024), 18374–18402. https://doi.org/10.3934/math.2024896

AIMS Press